

Bangs, Blips and Background: Decoding GRB Signals

Report

Rohit Kumar R

Contents

1 Abstract	1
2 Introduction	1
2.1 GRB Scientific Significance	1
2.1.1 Scientific uses	2
2.1.2 Cosmological Probes	2
2.2 AstroSat-CZTI Instrument.....	2
2.3 South Atlantic Anomaly (SAA)	3
3 Data Processing and Light Curve Construction	3
3.1 Data Structure	3
3.2 Light Curve Generation	3
4 Detrending Techniques	4
4.1 Savitzky-Golay Filter	4
4.2 Median Filter	4
4.3 Wavelet Denoising.....	5
4.4 Matched Filtering	6
4.5 Optimal Detrending Technique	6
5 Peak Detection and Validation.....	7
5.1 Signal-to-Noise Ratio Analysis.....	7
5.2 N-Sigma Thresholding	7
5.3 Spectrograms and energy-profile	8
5.3.1 Spectrograms	8
5.3.2 Energy Profile Analysis	8
6 Classification into Bang, Blips and Background	10
6.1 Bang - GRB	10
6.2 Blip - Charged particle.....	10
6.3 Background - Noise.....	11
7 Conclusion	12

1 Abstract

Gamma-Ray Bursts (GRBs) are among the most energetic events in the universe, providing deep insights into high-energy astrophysics. Using data from the Cadmium Zinc Telluride Imager (CZTI) onboard AstroSat (prompt emission), analyzed quadrant-level count-rate data to detect GRB signatures. The methodology involves masking data across multiple energy ranges (20-50 keV, 50-100 keV, 100-200 keV for CZT; 100-200 keV, 200-500 keV for Veto), applying denoising techniques (median filtering), implementing signal extraction algorithms employed peak detection via the n-sigma method and compute signal-to-noise ratios (SNR) to identify genuine transients while minimizing false positives and plotted the spectrogram to visualize the potential GRB energy profile and crosschecked whether it matches with the detected peak. This approach enables recovery of faint GRB signals typically obscured by noise and confirms previously unreported events during quiescent trigger periods. Results demonstrate CZTI's potential as a sensitive instrument for untriggered GRB detection and establish a framework for high-precision transient analysis in high-energy astrophysics.

2 Introduction

2.1 GRB Scientific Significance

Gamma-Ray Bursts (GRBs) are brief yet bright luminous flashes of gamma radiation, representing the most energetic electromagnetic events known in the universe. These bursts last from milliseconds to several minutes and are followed by multi-wavelength afterglows observable in X-ray, optical, and radio bands. GRBs are classified into two main types based on their duration and progenitors: long-duration GRBs ($\gtrsim 2$ seconds), typically associated with the core-collapse of massive stars, and short-duration GRBs ($\lesssim 2$ seconds), arising from the mergers of compact binaries such as neutron stars.

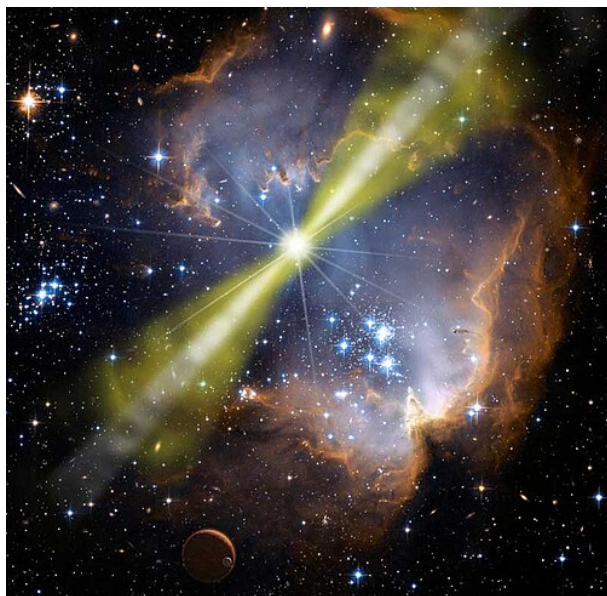


Figure 1: Long GRB following massive stellar collapse



Figure 2: Observed short GRB

GRB emission has two phases: the prompt phase, a brief, intense gamma-ray flash likely from internal shocks or magnetic reconnection, and the afterglow, caused by the jet interacting with the surrounding medium. While afterglows are easier to study and reveal jet and environment properties, the prompt phase is harder to capture due to its rapid variability and high energies.

Studying the prompt emission is particularly important as it provides direct insights into the physical processes at the heart of GRBs — such as jet composition (baryonic vs. Poynting-flux-dominated), radiation mechanisms (synchrotron vs. photospheric), and variability timescales. Yet, due to its short duration, rapid variability, and high photon energies, capturing the prompt phase with sufficient temporal and spectral resolution is technically challenging, making it a frontier in GRB research.

2.1.1 Scientific uses

GRBs serve as powerful probes of the distant universe. Their exceptional luminosity enables detection beyond redshift $z > 8$, providing windows into the early cosmic epochs. As GRB afterglows traverse the intergalactic medium (IGM), they imprint spectral signatures of intervening matter, allowing studies of IGM composition, ionization history, and metallicity evolution—particularly during the epoch of reionization. GRBs also offer potential pathways to detect Population III stars.

2.1.2 Cosmological Probes

While Type Ia supernovae serve as standard candles for distance measurements, their utility diminishes beyond $z \sim 2$. GRBs offer complementary standardizable candles through empirical correlations (Amati: E_p - E_{iso} ; Yonetoku: E_p - L_{iso} ; Ghirlanda: E_p - E_γ) that relate spectral peak energy (E_p) to isotropic energy (E_{iso}) or collimation-corrected energy (E_γ). Calibration of these relations could enable GRBs to constrain cosmological parameters (H_0 , Ω_m , w) and test Λ CDM, w_0w_a CDM, and modified gravity models.

2.2 AstroSat-CZTI Instrument

AstroSat, India’s first multi-wavelength space observatory (launched 2015), features the Cadmium Zinc Telluride Imager (CZTI) operating in the 20–200 keV range. CZTI’s wide field-of-view and off-axis sensitivity above 100 keV make it uniquely suited for GRB studies. The instrument comprises four quadrants (Q0–Q3) with CZT detectors overlaid by Veto detectors (100–500 keV) that suppress background events and cosmic rays.

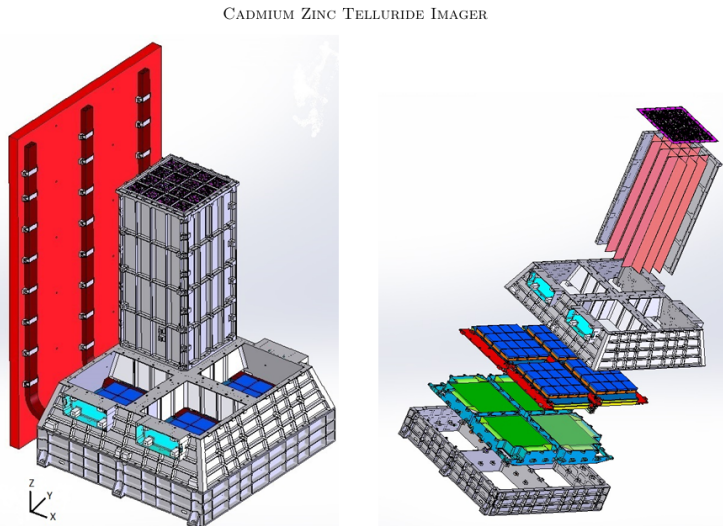


Figure 3: CZTI architecture: (Left) Four identical quadrants with detector housing (Right) CZT detectors (blue) and Veto detectors (green)

2.3 South Atlantic Anomaly (SAA)

The South Atlantic Anomaly (SAA) is a region where Earth's inner Van Allen radiation belt dips closest to the surface, causing elevated levels of high-energy particle radiation. Space-based X-ray and gamma-ray detectors (like those on Fermi, Swift, or AstroSat) experience:

- Increased background noise (false triggers)
- Higher detector dead time (reduced sensitivity)
- Degraded data quality (due to particle-induced signals)

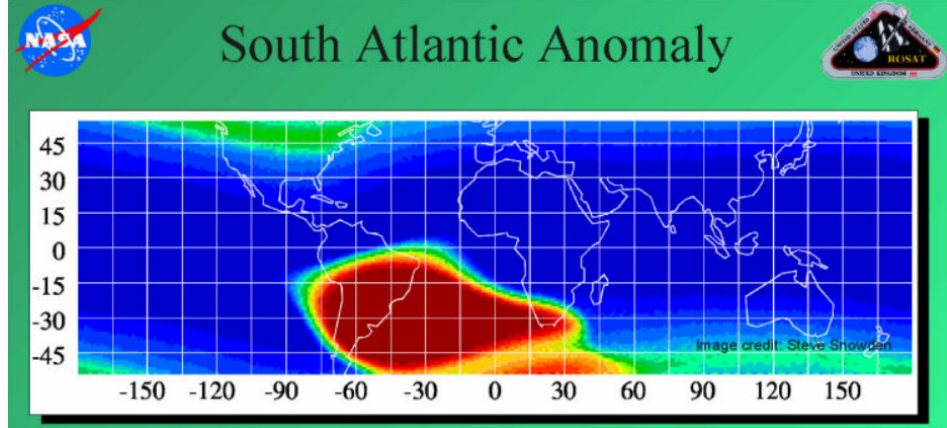


Figure 4: The SAA anomaly

The SAA has $10\text{--}100\times$ more charged particles (protons, electrons) than normal space regions. The extreme particle flux saturates the detector electronics. Many instruments disable data acquisition to prevent damage, leading to zero counts — which is exactly what happens with AstroSat.

So, masking out the SAA is a very important step to achieve proper GRB detection, as these data points with zero counts can ruin the median filter by giving false positives.

Having discussed the instrument and observational challenges like the SAA, we now move on to how the raw data from CZTI is structured and processed into meaningful light curves.

3 Data Processing and Light Curve Construction

3.1 Data Structure

Data were provided in FITS event files (.evt) containing time-tagged photon events. Using `astropy`, extracted metadata and detector-specific information. The hierarchical structure organizes data by quadrant (Q0-Q3 for CZT; VETOSPECTRUM for Veto), with columns including event time, energy, detector ID, and pixel coordinates (Figures 4,5).

3.2 Light Curve Generation

We generated light curves by binning events at 1s and 10s resolutions across energy bands:

- **CZT**: 20-50 keV, 50-100 keV, 100-200 keV
- **Veto**: 100-200 keV, 200-500 keV

```
In [2]: q1.columns
Out[2]: ColDefs(
    name = 'TIME'; format = 'D'; unit = 's'
    name = 'CZTSECCNT'; format = 'D'; unit = 's'
    name = 'CZTNTICK'; format = 'I'; unit = 'micro-sec'; bscale = 1; bzero = 32768
    name = 'PHA'; format = 'I'; unit = 'counts'; bscale = 1; bzero = 32768
    name = 'DetID'; format = 'B'
    name = 'pixID'; format = 'B'
    name = 'DETX'; format = 'B'
    name = 'DETY'; format = 'B'
    name = 'veto'; format = 'I'; unit = 'counts'; bscale = 1; bzero = 32768
    name = 'alpha'; format = 'B'; unit = 'counts'
    name = 'PI'; format = 'I'; bscale = 1; bzero = 32768
    name = 'ENERGY'; format = 'E'
)
```

Figure 4: CZT quadrant data structure

```
: veto.columns
: ColDefs(
    name = 'Time'; format = 'D'; unit = 's'
    name = 'CZTSECCNT'; format = 'D'; unit = 's'
    name = 'VetoSpec'; format = '256I'; bscale = 1; bzero = 32768
    name = 'QuadID'; format = 'B'
)
```

Figure 5: Veto detector data structure

Differential energy banding accounts for spectral variability in GRBs, where some events manifest predominantly in specific energy regimes. Temporal binning optimization is critical: finer bins (1s) resolve short bursts but increase noise, while coarser bins (10s) enhance signal-to-noise for weaker/longer events. Quadrant-level light curves enable cross-verification of astrophysical signals.

With the light curves generated, the next crucial step is to clean the data using denoising techniques that help isolate true astrophysical transients from background noise.

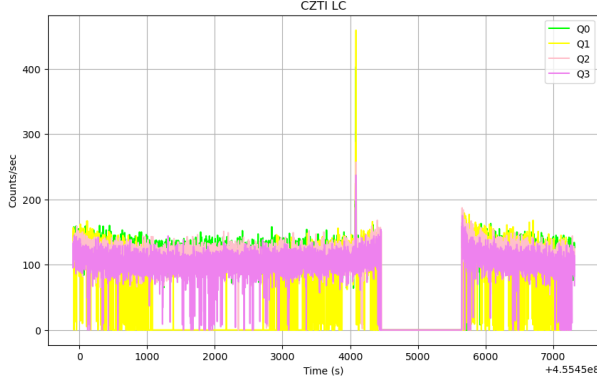


Figure 6: CZTI quadrant light curves showing count rate variations in different quadrants across time.

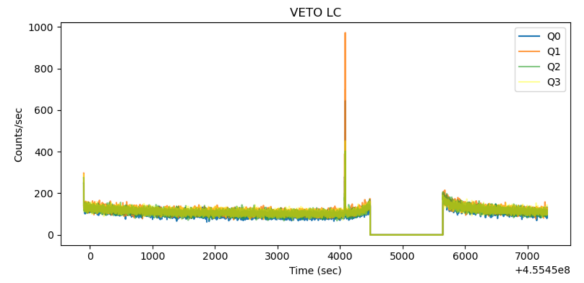


Figure 7: Veto detector light curves used for cross-verification of transient events and background noise suppression.

4 Detrending Techniques

4.1 Savitzky-Golay Filter

This filter applies local polynomial regression to preserve signal features while suppressing high-frequency noise. We observed peak attenuation and artificial negative values due to its Gaussian noise assumption (Figure 9), limiting its utility for quantitative SNR analysis despite providing adequate visualization.

4.2 Median Filter

As a nonlinear filter, the median filter replaces each point with the local median, effectively removing impulsive noise while preserving edges. It outperformed polynomial methods in retaining sharp GRB profiles (Figure 11) but may oversmooth structured backgrounds padded using the edge mode.

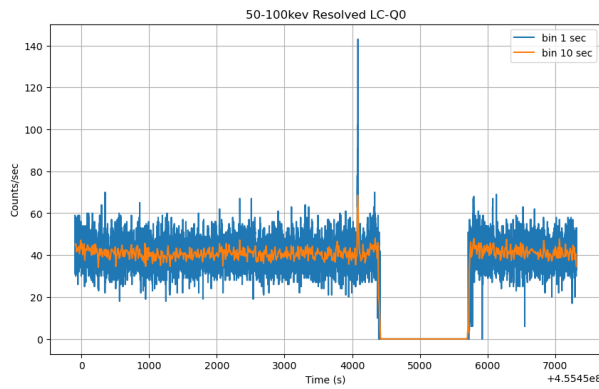


Figure 8: Raw light curve of Q0 (50–100 keV) with 1s and 10s bins, revealing transient variability.

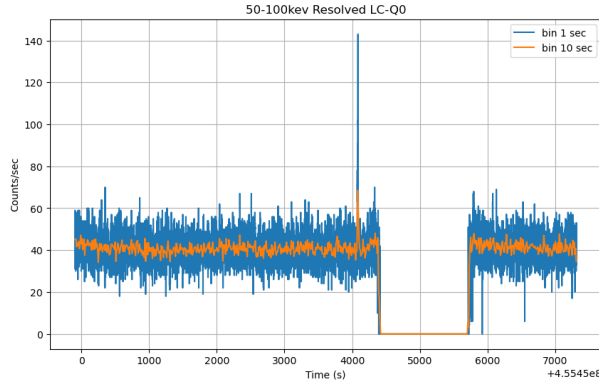


Figure 10: Raw Q0 light curve re-binned for clarity before applying the median filter.

4.3 Wavelet Denoising

Employing multiresolution analysis, wavelet decomposition separates signal from noise in time-frequency space. The discrete wavelet transform (symlet-5 basis) with universal thresholding yielded optimal noise suppression while preserving transient features (Figure 13). Residual plots quantitatively validated background removal.

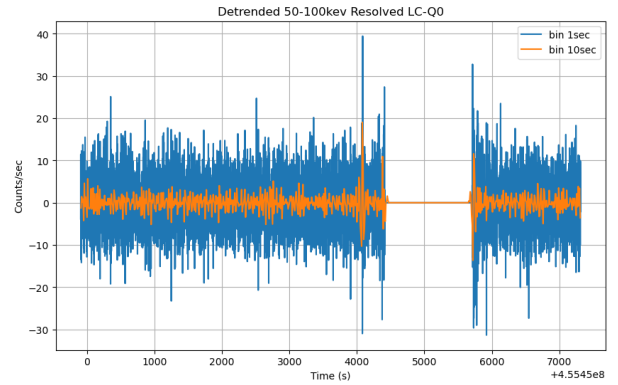


Figure 9: Savitzky-Golay filter output on Q0 data; smooths noise but suppresses peak amplitudes, unsuitable for GRB analysis.

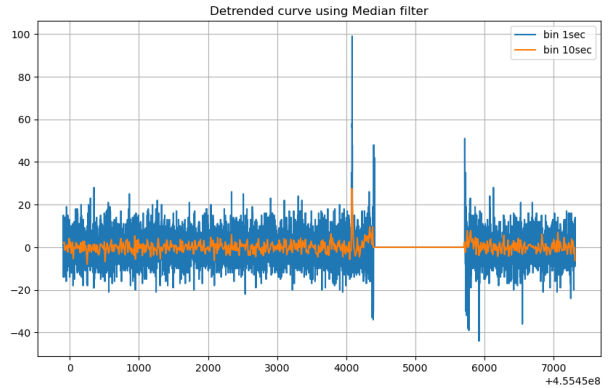


Figure 11: Median filter result for Q0; preserves sharp GRB-like peaks while suppressing spurious noise.

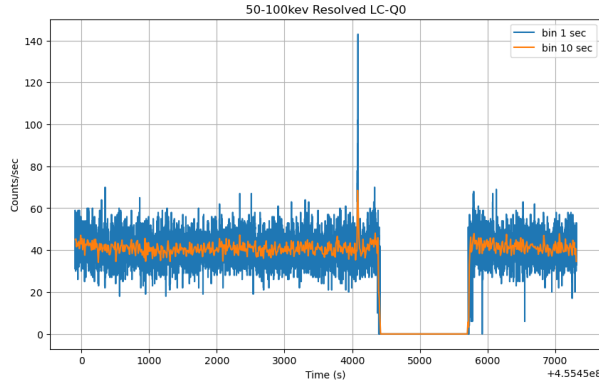


Figure 12: Original Q0 light curve for wavelet denoising comparison.

4.4 Matched Filtering

We implemented template matching using a Gaussian kernel ($\sigma = 2$ s) approximating GRB pulses. Cross-correlation peaked at potential burst locations (Figure 5B), but performance varied across energy bands due to template mismatch and weak signals.

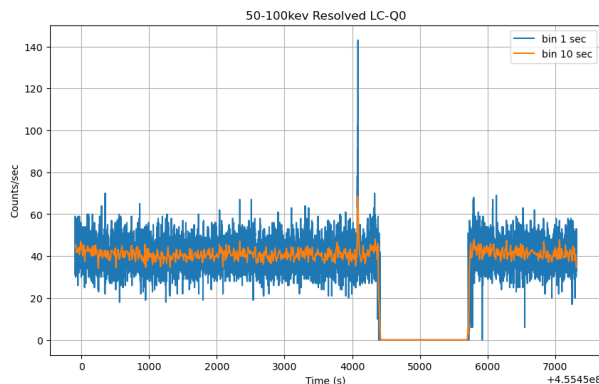


Figure 14: Raw Q0 light curve used to test matched filtering with Gaussian template.

4.5 Optimal Detrending Technique

Matched filtering, while theoretically optimal for known templates, performed poorly in our case due to GRB shapes differing from Gaussian kernels.

Likewise, Savitzky-Golay and wavelet denoising methods were suboptimal due to their tendency to smooth sudden peaks typical of GRB events.

The best choice was median out of all as it is good in capturing the outliers and are non linear.

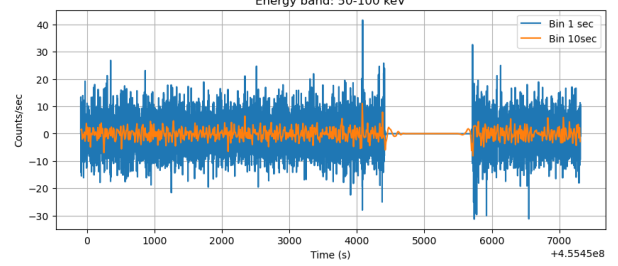


Figure 13: Wavelet-denoised light curve of Q0 showing better noise suppression but with some smoothing of transient features.

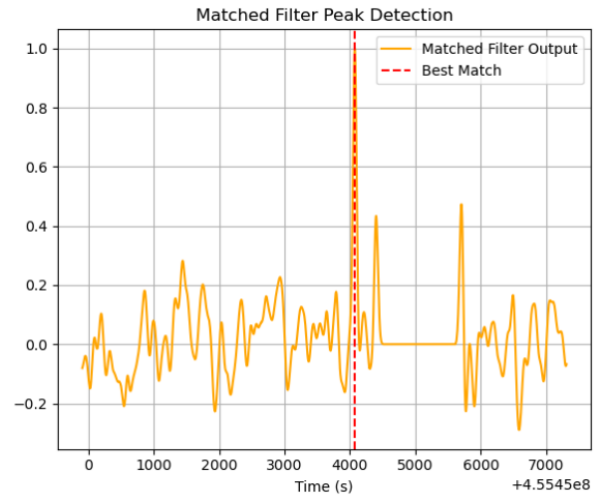


Figure 15: Matched filter response curve showing correlation peaks, but not robust across all energy bands.

5 Peak Detection and Validation

5.1 Signal-to-Noise Ratio Analysis

Computed SNR on detrended light curves:

$$\text{SNR} = \frac{S - B}{\sqrt{B}}$$

where S is raw signal and B is denoised background. Negative SNR values indicate sub-background fluctuations.

Once the data is detrended, we need to identify significant peaks that could correspond to real events. This section covers the statistical methods used to validate such peaks.

5.2 N-Sigma Thresholding

We implemented a 5σ detection criterion on denoised light curves:

$$\text{Detection} = \begin{cases} 1 & \text{if } C_i > \mu_b + 5\sigma_b \\ 0 & \text{otherwise} \end{cases}$$

where C_i is count rate, μ_b and σ_b are background mean and standard deviation. A transient at $t = 455454084$ s was identified across multiple quadrants and energy bands (Figures 6A-6H), satisfying astrophysical signal criteria (multi-quadrant coherence, energy-dependent profile).

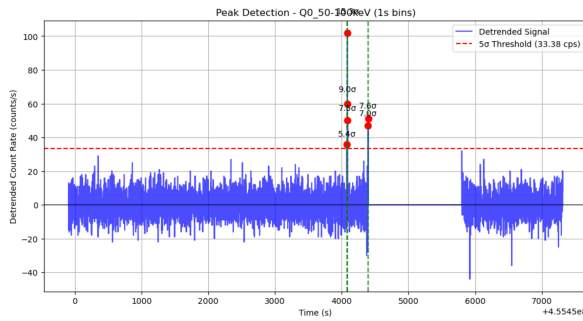


Figure 16: Peak detection: CZT Q0 (50-100 keV)

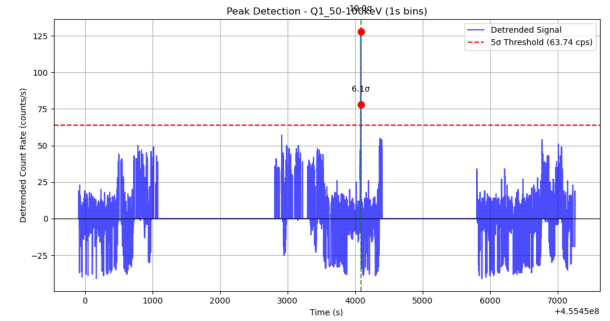


Figure 17: Peak detection: CZT Q1 (50-100 keV)

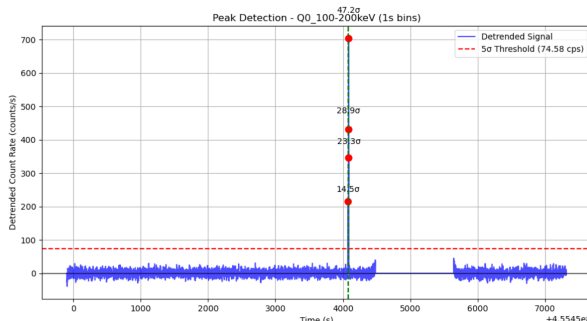


Figure 20: Peak detection: Veto Q0 (100-200 keV)

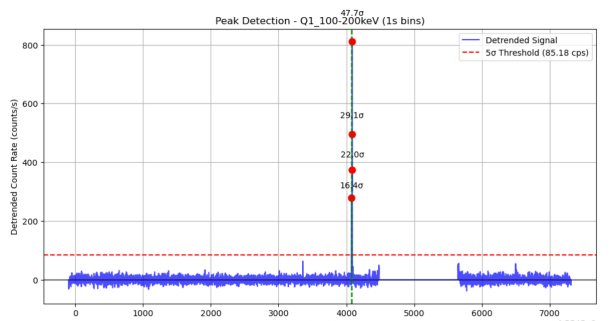


Figure 21: Peak detection: Veto Q1 (100-200 keV)

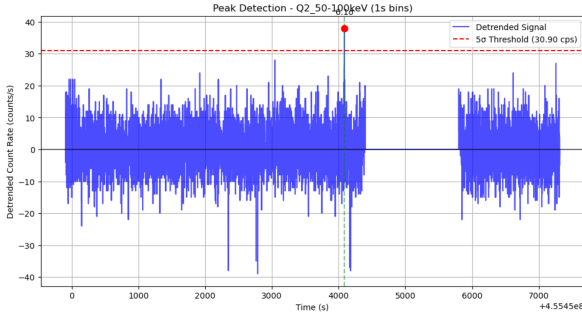


Figure 18: Peak detection: CZT Q2 (50-100 keV)

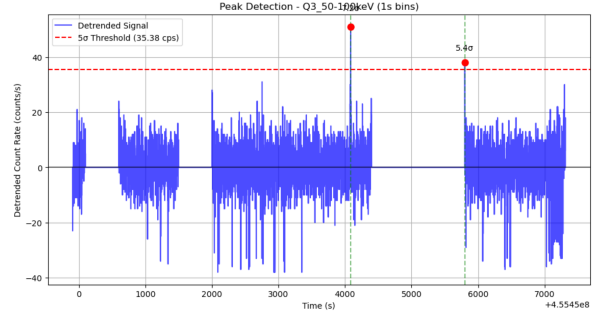


Figure 19: Peak detection: CZT Q3 (50-100 keV)

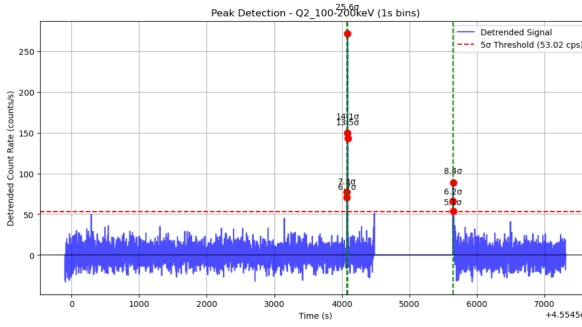


Figure 22: Peak detection: Veto Q2 (100-200 keV)

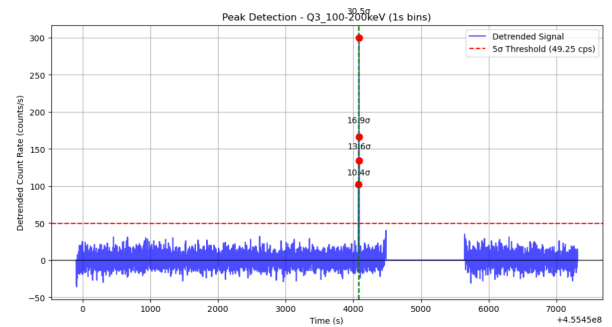


Figure 23: Peak detection: Veto Q3 (100-200 keV)

5.3 Spectrograms and energy-profile

5.3.1 Spectrograms

Shows how photon energies evolve with time across a burst window. By plotting energy vs. time, weighted by detrended counts, we can visually confirm short or long-duration GRBs and any spectral evolution (e.g., hard-to-soft behavior).

This is crucial to differentiate real transients from instrumental noise or cosmic rays. A window of +10 sec is taken around the potential GRB that is been detected from the nsigma thresholding and been analyzed.

5.3.2 Energy Profile Analysis

Enables Spectral Diagnostics. extracted photon counts across defined energy bands (20–50 keV, 50–100 keV, 100–200 keV) during both the event window and the background window.

This helps identify whether there's significant energy-dependent enhancement — a key indicator of a GRB rather than noise or background fluctuation. It is been considered that a GRB follows the power law in different energy ranges.

Not every peak in the light curve corresponds to a genuine GRB. To make sense of the detected events, we classify them based on physical characteristics and detection signatures.

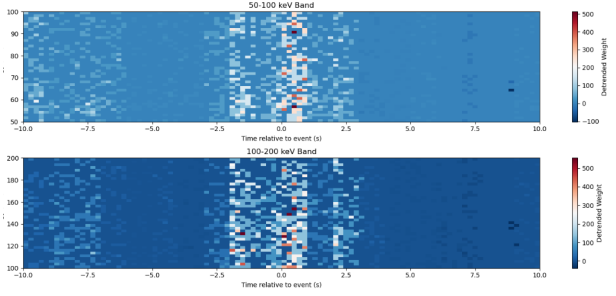


Figure 24: 10s window spectrogram for Q1 in 50–100 keV and 100–200 keV; shows energy evolution of the burst.

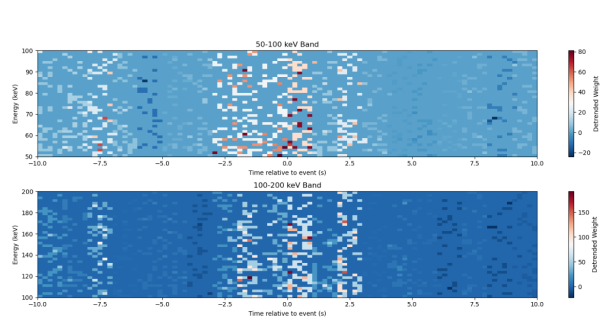


Figure 25: Similar 10s window spectrogram for Q2, confirming energy-dependent GRB signal structure.

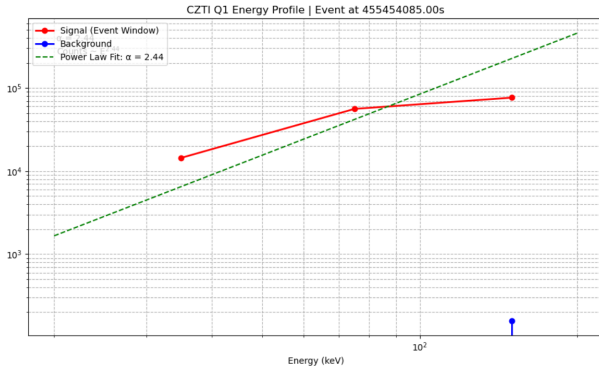


Figure 26: Energy profile for Q1 in three bands; clear power-law behavior supports astrophysical nature of event.

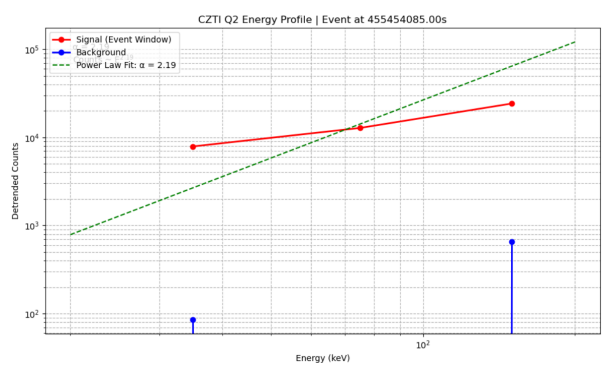


Figure 27: Energy profile for Q2; signal points deviate strongly from background and follow a power-law shape.

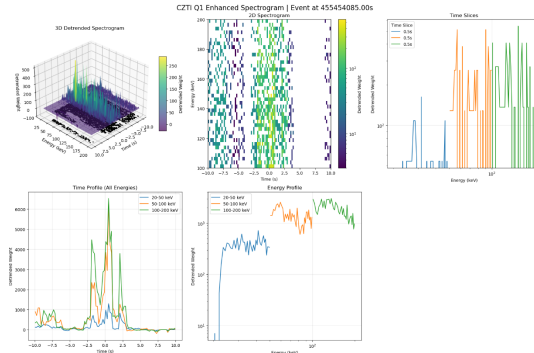


Figure 28: Enhanced 3D spectrogram visualization across time, energy, and intensity confirming structured GRB evolution..

6 Classification into Bang, Blips and Background

Not all spikes in the light curve correspond to GRBs; some may be charged particles or random background fluctuations. Accurate classification is essential to distinguish real astrophysical events.

To do so first from the results of the nsigma threshold were taken as it detected a number of peaks. With a certain threshold clustering of peaks wrt time were done using the DBSCAN clustering(based on time proximity).

The post-SAA (South Atlantic Anomaly) recovery time was also considered, as this period can produce numerous false positives in GRB and charged particle detections. During SAA passages, data often contain NaN values or noisy segments, and when a median filter is applied immediately after the SAA, these gaps can result in artificial spikes with high sigma significance. To mitigate this, events occurring within the defined post-SAA recovery window are automatically flagged as noise.

6.1 Bang - GRB

As GRBs are identified as sudden, intense increases in high-energy photon counts across multiple energy bands. In the pipeline, a “bang” refers to the potential detection of such a transient event, characterized by statistically significant peaks. For an event to be flagged as a GRB candidate, several conditions must be satisfied:

- **Multi quadrant and Multi-band Coincidence:** Peaks must be present in at least two adjacent energy bands (e.g., 50-100 keV and 100-200 keV) within a narrow temporal window and more than two quadrants. This reduces false positives caused by random fluctuations or single-energy anomalies.
- **Significance Threshold:** The peak should exceed a predefined sigma threshold (typically $> 5\sigma$ above the local background), calculated using the median-filtered baseline to ensure robustness against noise.
- **Time Profile Structure:** The event should exhibit a non-random temporal structure, typically a fast rise followed by an exponential decay distinguishing it from cosmic rays or instrumental noise.

Only when all of these criteria are met does the system flag an event as a genuine GRB candidate.

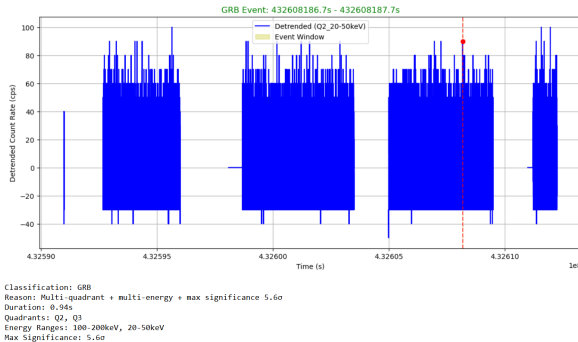


Figure 29: GRB detected with duration of 0.94s and 5.6σ significance; sharp peak confirmed on zooming into the event window.

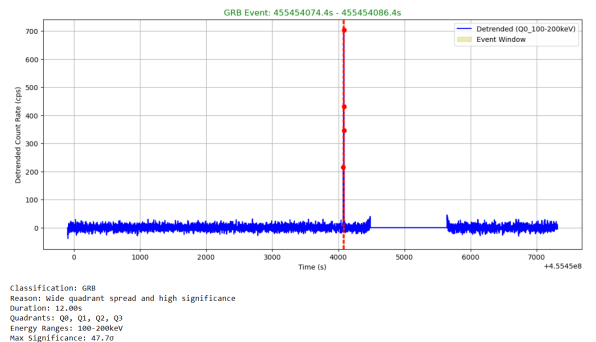


Figure 30: Strong GRB candidate detected across all CZT quadrants, satisfying multi-band and multi-quadrant criteria.

6.2 Blip - Charged particle

A ”blip” refers to a transient feature in the light curve that exhibits a localized increase in count rate but does not satisfy the full set of GRB conditions. These events may arise from charged particle hits or weak

astrophysical transients. The following criteria are used to classify an event as a blip:

- **Single-band Detection:** The peak is generally observed in only one energy band and in a single quadrant mostly, lacking the multi-band coherence typical of GRBs.
- **Marginal Significance:** The peak typically lies between 3σ and 5σ above the local background, indicating it is statistically noticeable but not strong enough to be confidently considered a GRB. But some cases there can be significance more than 5σ in figure 31 and 32
- **Narrow Duration:** Most blips last for only a few bins (often ≤ 1 second), without the structured evolution seen in genuine bursts.

Blips are retained in the analysis for further inspection or potential astrophysical classification but are distinguished from high-confidence GRB detections.

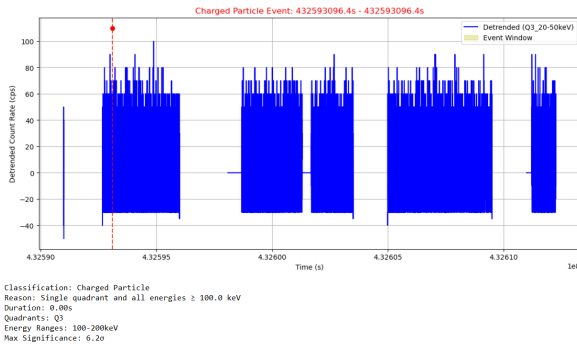


Figure 31: Charged particle blip seen only in Q3 at 100–200 keV with short duration and 6.2σ peak — no multi-band match.

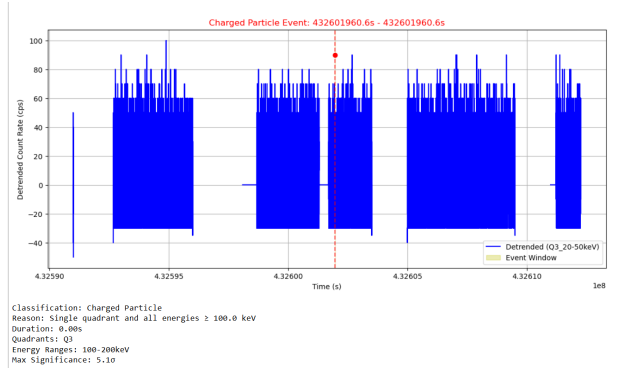


Figure 32: Another blip in Q3 with 5.1σ , again lacking spectral or temporal structure to qualify as a GRB.

6.3 Background - Noise

”Noise” events typically are caused by instrumental effects, statistical fluctuations, or contamination from the SAA and other background features. These are explicitly excluded from further consideration. The key identifiers of noise events include:

- **Noisy or Fluctuating Baseline:** Noise events often emerge from unstable background trends rather than clear, isolated peaks.
- **Sub-threshold Significance:** Peaks do not exceed the 3σ threshold above the local median, making them statistically consistent with random fluctuations.
- **No Temporal or Spectral Structure:** The absence of rise-decay morphology, consistent duration, or energy-based features clearly separates noise from astrophysical signals (as in Fig 33).
- **Single-frame or Nan-associated Glitches:** Events occurring in regions immediately after large NaN spans (e.g., post-SAA recovery) or involving sudden single-bin spikes are automatically flagged as noise due to high false-positive risk (as in Fig 34).

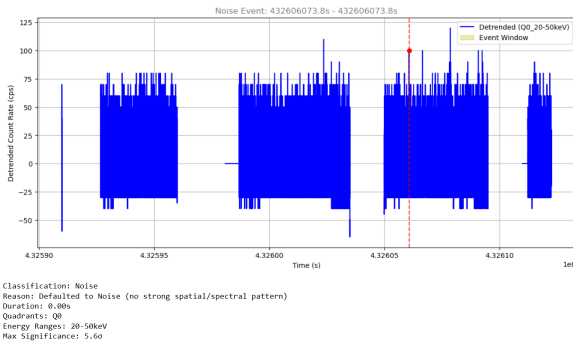


Figure 33: Noise event without spectral pattern or structure — zoomed-in view confirms lack of GRB signature.

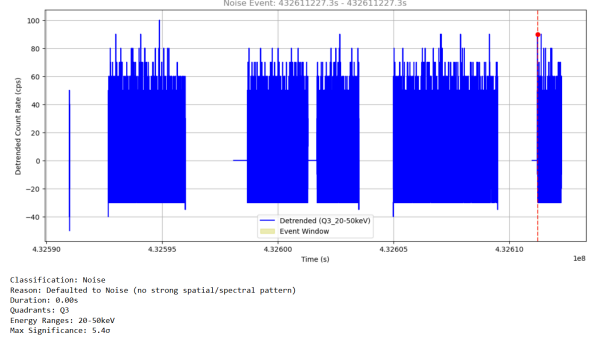


Figure 34: Automatically flagged noise event immediately post-SAA; likely a false positive caused by filter artifacts.

7 Conclusion

The developed pipeline successfully detects and classifies transient events in AstroSat-CZTI data into GRBs, charged particle, and background noise. By implementing a combination of median filtering, Nsigma threshold, energy profile analysis, and spectrogram validation, the framework reliably distinguishes bursts from noise and artifacts. This structured classification lays the foundation for automated large-scale transient studies. As a future extension, I aim to build a machine learning classifier trained on this labeled dataset, allowing for real-time classification and cross-instrument verification.

References

The following webs and papers were referred to while preparing this report but are not cited in the main text:

- GRB Wikipedia including images.
- **M. G. Dainotti, B. De Simone, G. Montani, E. Rinaldi, M. Bogdan, K. M. Islam, A. Gangopadhyay** arXiv:2309.05876
- **Marek Demianski, Ester Piedipalumbo, Disha Sawant, Lorenzo Amati** A&A 598, A112 (2017)
- **F. Y. Wang, Z. G. Dai, E. W. Liang** arXiv:1504.00735
- **Davide Lazzati, Gabriele Ghisellini, Francesco Haardt, Alberto Fernandez-Soto** arXiv:astro-ph/0103307v1
- **F. Y. Wang, Z. G. Dai, E. W. Liang** arXiv:2203.04610
- **Bhalerao, V. search by orcid ; Bhattacharya, D. search by orcid ; Vibhute, A. ; Pawar, P. ; Rao, A. R. ; Hingar, M. K. ; Khanna, Rakesh ; Kutty, A. P. K. ; Malkar, J. P. ; Patil, M. H. ; Arora, Y. K. ; Sinha, S. ; Priya, P. ; Samuel, Essy ; Sreekumar, S. ; Vinod, P. ; Mithun, N. P. S. ; Vadawale, S. V. search by orcid ; Vagshette, N. ; Navalgund, K. H.** ui.adasabs.harvard.edu
- SAA Wikipedia
- **Kulinder Pal Singh** arXiv:2203.04610

- **Neal Gallagher** Savitzky Golay Smoothing
- **Aminou Halidou, Youssoufa Mohamadou, Ado Adamou Abba Ari Edinio Jocelyn Gbadoubissa Zacko** Wavelet Denoising Article
- **Roberto Vio, Paola Andreani** arXiv:2107.09378
- **David Gruber, Adam Goldstein, Victoria Weller von Ahlefeld, P. Narayana Bhat, Elisabetta Bissaldi, Michael S. Briggs, Dave Byrne, William H. Cleveland, Valerie Connaughton, Roland Diehl** iop.science